CHAPTER III

VALIDATION OF THE ESTIMATION OF CORNEAL ABERRATIONS FROM VIDEOKERATOGRAPHY: A TEST ON KERATOCONUS EYES

This chapter is based on the article by Barbero, S, et al., *A validation of the estimation of corneal aberrations from videokeratography: test on keratoconus eyes.* J Refract Surg, 2002. 18: p. 267-270. Coauthors of the study are: Susana Marcos, Jesus Merayo-Lloves and Esther Moreno-Barriuso.

The contribution of Sergio Barbero to the study was to develop the corneal aberrations technique, to carry out the experimental measurements (total and corneal aberrations) on patients, data analysis, and the discussion of the results.

RESUMEN

OBJETIVOS: Validación de una técnica de trazado de rayos virtual, a partir de datos de elevación de un topógrafo corneal, comparando los resultados con una técnica de trazado de rayos experimental (LRT) para la medida de aberraciones totales, en ojos donde domina la óptica de la cornea (i.e. queratocono). Estudio de las aberraciones ópticas en ojos con queratocono.

MÉTODOS: Medimos las aberraciones totales y corneales en 3 ojos diagnosticados con queratocono mediante el examen clínico con una lámpara de hendidura y topografía corneal. Dos de los ojos de uno de los pacientes (A) manifestaban queratoconos incipiente, mientras en un ojo de otro paciente (B) el queratocono se encontraba en un estado avanzado. Las medidas de aberraciones totales se realizaron con la técnica de trazado de rayos (LRT). Las aberraciones corneales se calcularon a partir de datos de elevación tomados con un topógrafo corneal (modelo Humphrey Instruments) mediante una marcha de rayos virtual.

RESULTADOS: 1) Los ojos con queratocono medidos muestran una cantidad significativamente mayor de aberraciones (tanto totales como corneales) ―especialmente aberraciones de tipo comático― que las de un grupo de ojos normales (3.74 veces mayor en promedio). 2) El mapa de aberración total y corneal es muy similar en ojos con queratocono. 3) Esta similitud es mayor en el paciente A, lo cual podría ser indicativo de una contribución significativa de la cara posterior de la cornea en el paciente B.

CONCLUSIONES: 1) La semejanza en los patrones de aberraciones totales y corneales encontradas en los pacientes con queratocono sirve como una prueba de validación de ambas técnicas para ser usadas conjuntamente. 2) Ambas técnicas son útiles en el diagnóstico y cuantificación de la degradación óptica debido al queratocono.

ABSTRACT

PURPOSE: To validate the estimation of corneal aberrations from videokeratography against a laser ray tracing technique (LRT) that measures total eye aberrations, in eyes with cornea-dominated wave aberrations (i.e. keratoconus). To study optical aberrations in eyes suffering keratoconus.

METHODS: We measured total and corneal wave aberrations of 3 eyes diagnosed with keratoconus by slit-lamp microscope examination and corneal topography: two eyes from one patient (A) with early keratoconus and one eye with a more advanced keratoconus (B). Total aberrations were measured with LRT. Corneal aberrations were obtained from corneal elevation data measured with a Humphrey Instruments corneal videokeratoscope, and using custom software that performs a virtual a ray tracing on the measured front corneal surface. RESULTS: 1) The keratoconus eyes show a dramatic increase in aberrations (both corneal and total) particularly coma-like terms respect of a group of normal eyes (3.74 times higher on average). 2) Anterior corneal surface aberrations and total aberrations are very similar in keratoconus. 3) This similarity is greater for patient A, suggesting a possible implication of the posterior corneal surface in patient B. CONCLUSIONS 1) The similarity found between corneal and total aberration patterns in keratoconus provides a cross-validation of both types of measurements (corneal topography and aberrometry 2) Both techniques are useful in diagnosing and quantifying optical degradation imposed by keratoconus.

1. Introduction

While the presence of optical imperfections in the eye beyond conventional refractive errors (known as optical aberrations) have been noticed for more than a century[1], it is only in the last few years when they have been considered from a clinical perspective. The interest has been mainly drawn by the evaluation of refractive surgery outcomes, and by the increasing possibilities of correcting (through surgery or other means) these high order errors[2-4].   Corneal topography systems are widely used in the clinic, and in particular, corneal aberrations have been measured following refractive surgery, and the results have been correlated to visual performance[5, 6]. However, the optical quality of the human eye is determined by the optical properties of both the cornea and the lens, as well as to their relative alignment and to the position of the pupil[7]. For this reason the measurement of the total aberrations provides the most complete description of the image forming properties of the eye.

Several types of aberrometers have been used to assess the ocular aberrations in normal eyes[8-10], and following refractive surgery[11-14]. Undoubtedly, the combination of the information provided by corneal topography and aberrometry provides interesting insight into the properties of the individual ocular components[14-16]. However, both techniques rely on very different principles. Typical corneal topographers project a Placido disk (a set of concentric rings) onto the anterior surface of the cornea. Corneal elevation maps are obtained from the distortions of the reflected rings. The aberrations caused by the front surface of the cornea are then computed by theoretical ray tracing. However, typical aberrometers measure the deviations of beams projected onto the retina through different pupil locations (i.e. laser ray tracing[17], spatially resolved refractometer[18] or Tscherning´s aberroscope[19]), or analyze the wavefront as it emerges out of the eye (i.e. Hartmann-Shack[8]). Factors affecting resolution and accuracy are very different across methods (videokeratography and aberrometry). Whereas the wave aberration is computed directly from a set of ray aberrations, the corneal heights are computed from the ring reflection positions and surface location measured from the video images[20]. Total aberrations are measured directly, whereas some assumptions (i.e. index of refraction) are needed to compute corneal aberrations.

Prior to comparing total and corneal aberrations, it seems necessary to prove that both techniques are directly comparable. The ideal test are eyes where total and corneal aberrations should be identical, or at least eyes where total aberrations are dominated by the aberrations of

the front surface of the cornea. An approximate model of the first case is an aphakic eye. An approximate model of the second is a keratoconus. Given the distinct nature of the two cases, we will treat them separately. In the current chapter, we will study the keratoconus case –the aphakic case will be study in chapter IV-.

The front surface of the cornea is the major refractive component in the eye, and it is strongly distorted in eyes suffering from keratoconus[21, 22]. Important similarities are therefore to be expected between anterior corneal aberration and total aberration patterns. Furthermore, this comparison can be a good cross-validation of the two techniques used in this study: 1) Computation of anterior corneal aberrations by simulated ray tracing on corneal elevation maps as measured by a Humphrey Atlas corneal videokeratoscope, and 2) Laser Ray Tracing measurements of ocular aberrations. Although presumably relatively small in conventional keratoconus, the crystalline lens and posterior corneal surface play a role in overall image quality[15, 23]. This indicates that the measurement of total aberrations may have advantages over the measurement of just anterior corneal aberrations, allowing a better comparison with visual performance. For example, posterior keratoconus, characterized by a conical protrusion of the posterior corneal curvature, a thinned stroma and non-protruding anterior surface[24], could be detected measuring the total aberrations, while anterior aberrations would appear as normal. A lack of correspondence between total and anterior corneal aberrations in a diagnosed keratoconus may well be indicative of an involvement of the posterior corneal surface.

2. Patient and methods

Total and corneal aberrations were measured on three eyes from two patients: both eyes of patient A (female, aged 34) and right eye of patient B (female, age 40). The three eyes were diagnosed with keratoconus by slit-lamp microscope examination, corneal topography, presence of high astigmatism, and reduced visual acuity, being in an early stage for patient A and more advanced in patient B. Computer-assisted videokeratography (Humphrey-Zeiss Mastervue Atlas Corneal Topography system) was performed during the experimental sessions. Figure III.1 shows topographic power maps, revealing corneal inferior steepening in all eyes within ranges reported in the literature as indicative of keratoconus[21, 25, 26].

Patient A   **Patient B**

　　OD　　　　　　　　　　**OS**　　　　　　　　　　**OD**
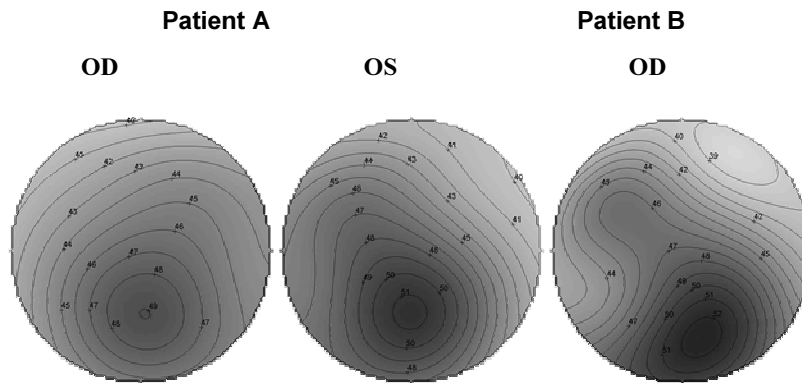
Figure III.1: Topographic power maps, revealing corneal inferior steepening in all eyes within ranges reported in the literature as indicative of keratoconus[21, 25, 26].

Patient A's autorefractometer refraction was –2.5D –2.5D x 35º (OD) and –2D –2D x 125º (OS). Best spectacle-corrected visual acuity (BSCVA) was 20/50 and 20/40 respectively. Patient B's refraction was –5.25D –5.25D x 33º (OD), with a BSCVA of 20/100. The two types of measurements (corneal and total aberrations) were performed in the same experimental session, after recent clinical screening. Pupils were dilated with one drop of tropicamide 1%. The patients signed informed consent forms approved by institutional ethical committees.

Total aberrations were measured using a Laser Ray Tracing (LRT) Technique Figure III.2 (a) shows the set of retinal images for one of the runs recorded in a keratoconus eye (Patient A, OD). The location indicates the corresponding entry pupil position. Measurements were done over a 6.51 mm effective pupil diameter for patient A (step-size= 1-mm) and 5.5 mm for patient B (step-size=0.8-mm). We had to reduce slightly the sampled area due to the large amount of aberrations present in patient B. Even with best spherical and cylindrical correction, the aerial images for the most eccentric locations of 6.51 mm pupil did not fit in the CCD array. Figure III.2 (b) shows a joint plot of the centroids of those images (spot diagram).
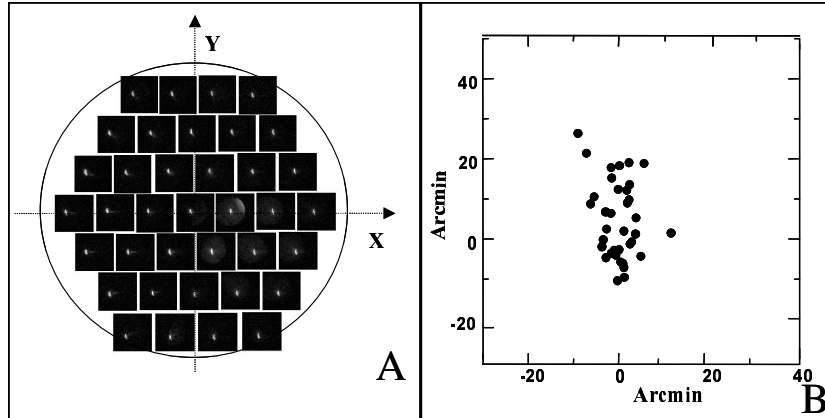
Figure III.2: A) Set of retinal images, captured by the high resolution CCD in Laser Ray Tracing as a function of entry pupil location, for patient A, OS. Each retinal aerial image is located at the corresponding entry pupil location. Pupil effective diameter was 6.51 mm. **B)** Spot diagram, i.e. joint plot of centroids of the retinal images shown in A.

Corneal elevation maps were obtained from each eye, using the Mastervue Corneal Topography System (Humphrey Instruments, San Leandro, CA). Except for initial control experiments, only one map was captured per eye. Figure III.3 (a) shows a typical corneal elevation map in a keratoconic eye (Patient A, OS). In order to show the irregularities, we have subtracted the first six terms of Zernike polynomial fit to the height data from the raw height data[27]. Figure III.3 (b) shows the simulated spot diagram for the example shown in Figure III.3 (a).
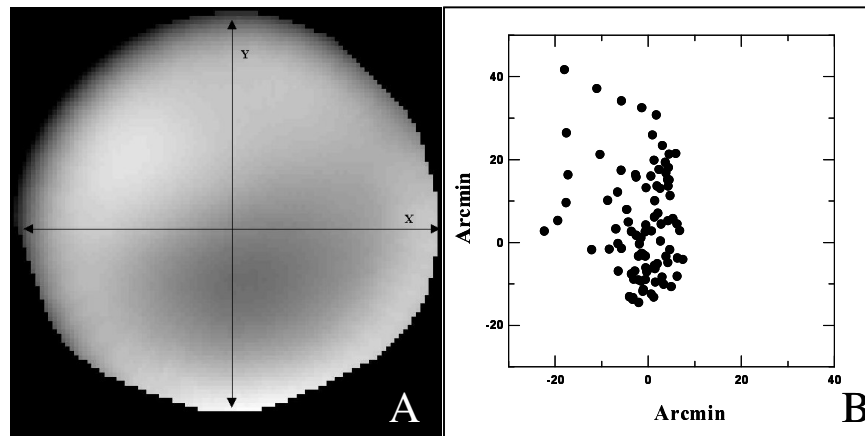
Figure III.3: A): Residual height map of patient A, OS. A Zernike polynomial fitting (up to the 2nd order) has been substracted from raw height data, in order to enhance relevant features[27]. **B)** Spot diagram obtained by virtual ray tracing on corneal height data (Patient A, OS). Stop pupil diameter was 6.51 mm after appropriate centration.

3. Results

Figure III.4 shows total (upper row) and corneal (lower row) wave aberration maps for patients A (OD and OS) and B (OD). Contours have been plotted at 1-µm intervals. Pupil sizes are 6.51-mm for patient A and 5.5-mm for patient B. The gray scale for corneal and total aberrations is the same for each patient. Tilt and defocus have been cancelled in all eyes.

There is a good correspondence between corneal and total wave aberration maps. Peak-to-valley values are double in patient B than in patient A.

Figure III.5 compares corneal (open diamonds) and total (solid circles) Zernike coefficients for each eye, following the ordering and notation recommended by the Optical Society of America Standard Committee[28]. For patient A, there is a good correspondence between total and corneal aberrations. In both eyes of this subject, the dominant aberration is the coma term Z_3^{-1}, which is higher than astigmatism. The dominance of coma is also evident in the wave aberration plots.
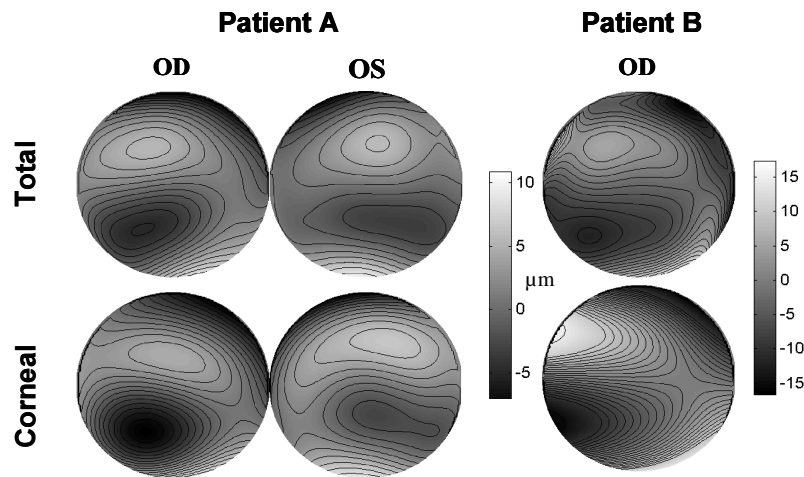
Figure III.4: Wave aberration patterns (without tilts and defocus) in the 3 measured eyes, for total aberrations (upper row) and corneal aberration (lower row). Contour lines are plotted every 1 µm. The grey scale pattern represents wave aberration heights in microns. Diameters were 6.51 mm in patient A and 5.51mm in patient B.
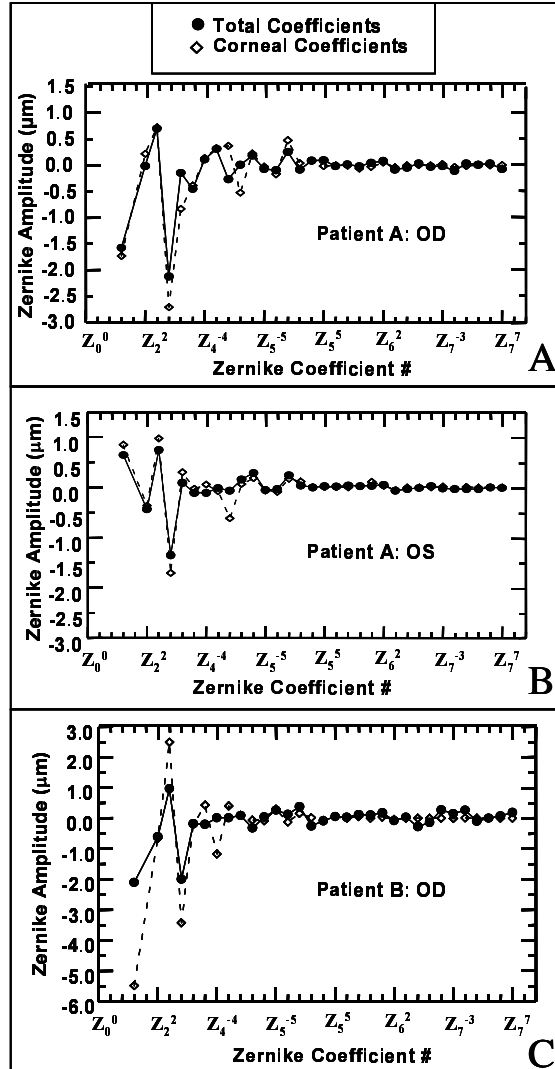
Figure III.5: Total (solid circles) and corneal (empty diamonds) aberrations for Patient A, OD (A), Patient A, OS (B) and Patient B, OD (C). Notation follows the OSA Standard Committee's recommendations[28]

The largest difference between total and corneal aberration for patient A was found for spherical aberration (coefficient of Z_4^0 element). For the right eye, corneal and total spherical aberration have different sign and show a total difference of 0.74 µm, whereas for the left eye corneal spherical aberration exceeds total spherical aberration by 0.55 µm. This indicates a compensation of corneal spherical aberration by spherical aberration of the crystalline lens. This balance of spherical aberration is a common finding in normal eyes[15, 29]. While the progressive disease seems to affect high order terms (particularly coma) of both corneal and total aberrations, it does not seem to modify the amount of spherical aberration (Z_4^0).

In patient B, the correspondence between corneal and total Zernike terms is worse than for patient A. Some exceptional terms show large differences. Major differences are found in astigmatic term Z_2^{-2} (4.58 µm difference), third order term Z_3^3 (0.63 µm) and 4th order term Z_4^{-4} (1.15 µm). In this subject, astigmatism is the dominant term, followed by coma.

For the sake of clarity, error bars have not been plotted in Figure III.5. Control experiments performed in one patient show a mean standard deviation of 0.08 µm for the corneal Zernike coefficients (averaged across terms, excluding tilts and defocus). The mean standard deviation for the total Zernike coefficients (averaging across the three eyes and coefficients) was 0.13 µm.

Table III.1 shows the RMS for different terms and orders evaluated for the three eyes. There is a clear predominance of 3rd order (coma-like) terms, both in corneal and total aberration. In terms of variance (squared RMS), they represent 61% (70.72% for patient A and 41.53% for patient B) of the aberration (excluding tilt and defocus, but including astigmatism). Excluding astigmatism, coma-like terms represent 90.85% of the variance. Mean 3rd order aberration (2.02±0.41 µm) in this group of keratoconus eyes exceeds by a factor of 3.74 the average 3rd order aberration (0.54±0.30 µm) of a group of normal eyes. This control group of 22 eyes from 12 subjects was within similar age range (28±5 years) and within similar refractive errors (-6.42±2.5 D sphere)[13].

	Patient A OD		Patient A OS		Patient B OD	
	Total	**Corneal**	**Total**	**Corneal**	**Total**	**Corneal**
Z_2^-	1.58	1.73	-0.64	-0.85	-2.1	-5.24
Z_2	0.01	-0.22	0.44	0.34	-0.6	-0.66
RMS 2rd to 7rd order (except defocus)	2.84	3.55	1.8	2.3	3.25	7.1
RMS 3 order	2.29	2.95	1.55	1.99	2.23	4.26
RMS 3&higher order	2.36	3.09	1.62	2.11	2.4	4.46
RMS 4 order	0.46	0.77	0.35	0.66	0.33	1.24
RMS 5&higher order	0.38	0.52	0.28	0.27	0.82	0.38
$\dfrac{\text{Variance } 3^{rd} *100}{\text{Var } 2^{rd}\&\text{Higher (no defocus)}}$	64.9	69.1	74.1	74.9	47.1	36
$\dfrac{\text{Variance } 3^{rd} *100}{\text{Var } 3^{rd}\&\text{Higher}}$	94.1	91.1	91.6	89	86.3	93

Table III.1: Root mean square (RMS) and Zernike corneal and total terms of OD-OS in patient A and OD in patient B.

4. Discussion

Corneal and total aberrations were estimated in three eyes, all diagnosed with keratoconus at different stages of the disease. We found good correspondence between corneal and total aberrations, particularly in both eyes of patient A, indicating that the overall aberration pattern is dominated by the front corneal surface, and that both methods are able to capture similarly the distortions produced by the irregular cornea. Our results show that Humphrey Mastervue Atlas corneal topography system and laser ray tracing are both adequate tools to analyze optical quality in keratoconus. As reported previously[30] image degradation in keratoconus is mainly due to an increase in higher order aberrations, particularly coma. In the three affected eyes from this study, third order aberrations increase by a factor of 4.24, 2.87 & 4.13 respectively with respect to normal eyes[13].

We have shown both techniques provided good results (valid topography data and good quality retinal images in LRT) in these eyes with abnormally high order aberrations. Both techniques failed in two eyes with a highly advanced stage of keratoconus (one patient scheduled for keratoplasty, not shown here). In these eyes, the videokeratographic images were so distorted that the commercial software did not accept the data. Many of the LRT aerial retinal images were highly diffused (probably due to corneal scarring), and even after compensation of spherical error they did not fit within the CCD area. There are many differences inherent to the techniques under use, and nevertheless the similarity of the corneal and total aberration pattern is high, at least for patient A. The accuracy of the measurements is determined by different factors (see chapter II). The fact that, despite these differences the results are similar, indicates that these factors do not seem to be essential.

In summary, we have crossed-validated two techniques for measuring corneal and total aberrations respectively with tests on eyes with keratoconus. They have proved powerful to detect and quantify the aberrations in moderate keratoconus. The data on patient B shown in this paper probably sets a limit where the assumptions of the techniques are valid to provide valid quantitative data. We had to use a smaller pupil diameter in the LRT system in order to capture the entire set of retinal images. Measurements in a very advanced keratoconus failed with both instruments. Finally, part of the differences found between specific terms of corneal and total aberrations in patient B might have been caused by the posterior corneal surface could being affected in advanced keratoconus[22]. In this regard, measurement of overall aberrations has advantages over corneal topography, since it allows capturing possible alterations of the posterior corneal surface. Since they contain information of all optical components (including the crystalline lens) they provide the most complete description of the imaging properties of the eye.

5. References

1. H. V. Helmholtz, *Physiological Optics* (J.P.C. Southhall, New York, 1896).
2. S. M. MacRae, J. Schwiegerling, and R. Snyder, "Customized corneal ablation and super vision," J Refract Surg 16(suppl), S230-S235 (2000).
3. J. Liang, D. Williams, and D. Miller, "Supernormal vision and high-resolution retinal imaging through adaptive optics," J Opt Soc Am 14, 2884-2892 (1997).
4. R. Navarro, E. Moreno, S. Bará, and T. Mancebo, "Phase-plates for wave-aberration compensation in the human eye," Opt. Lett. 25, 236-238 (2000).
5. S. Marcos, "Aberrations and visual performance following standar laser vision correction," J Refract Surg 18, 596-601 (2001).

6.   R. A. Applegate, G. Hilmantel, H. Howland, E. Y. Tu, T. Starck, and J. Zayak, "Corneal first surface optical aberrations and visual performance," J Refract Surg 16, 507-514 (2000).

7.   S. Marcos, S. A. Burns, P. M. Prieto, R. Navarro, and B. Baraibar, "Investigating the sources of monochromatic aberrations and transverse chromatic aberration," Vision Res 41, 3862-3871 (2001).

8.   J. Liang, B. Grimm, S. Golez, and J. Bille, "Objetive measurement of wave aberrations of the human eye with the use of a Hartmann-Shack wave-front sensor," J Opt Soc Am A 11(7), 1949-1957 (1994).

9.   R. Navarro and M. A. Losada, "Aberrations and relative efficiency of light pencils in the living human eye," Optom Vis Sci 74, 540-547 (1997).

10.   J. C. He, S. Marcos, R. H. Webb, and S. A. Burns, "Measurement of the wave-front aberration of the eye by a fast psychophysical procedure," J. Opt. Soc. Am. A. 15(9), 2449-2456 (1998).

11.   L. N. Thibos and X. Hong, "Clinical applications of the Shack-Hartmann aberrometer," Optom Vis Sci 76, 817-825 (1999).

12.   T. Seiler, M. Kaemmerer, P. Mierdel, and H.-E. Krinke, "Ocular optical aberrations after photorefractive keratectomy for myopia and myopic astigmatism," Arch Ophthalmol 118, 17-21 (2000).

13.   E. Moreno-Barriuso, J. Merayo-Lloves, S. Marcos, R. Navarro, L. Llorente, and S. Barbero, "Ocular aberrations before and after corneal refractive surgery: LASIK-induced changes measured with Laser Ray Tracing," Invest Ophthalmol Vis Sci 42, 1396-1403 (2001).

14.   S. Marcos, S. Barbero, L. Llorente, and J. Merayo-Lloves, "Optical Response to Myopic LASIK Surgery from Total and Corneal Aberration Measurements," Invest Ophthalmol Vis Sci 42, 3349-3356 (2001).

15.   P. Artal and A. Guirao, "Contribution of the cornea and the lens to the aberrations of the human eyes," Opt Lett 23, 1713-1715 (1998).

16.   T. Salmon and L. Thibos, "Relative balance of corneal and internal aberrations in the human eye," OSA Annual Meeting. Baltimore, Md, 1998. (1998).

17.   R. Navarro and E. Moreno-Barriuso, "Laser ray-tracing method for optical testing," Optics Letters 24(14), 1-3 (1999).

18.   J. C. He, S. Marcos, and S. A. Burns, "Comparison of cone directionality determined by psychophysical and reflectometric techniques," J Opt Soc Am A Opt Image Sci Vis 16(10), 2363-2369 (1999).

19.   M. Mrochen, M. Kaemmerer, P. Mierdel, H. E. Krinke, and T. Seiler, "Principles of Tscherning Aberrometry," J Refract Surgery 16, S570-S571 (2000).

20.   C. Campbell, "Reconstruction of the corneal shape with the MasterVue Corneal Topography System," Optom Vis Sci 74, 899-905 (1997).

21.   L. J. Maguire and W. M. Bourne, "Corneal topography of early keratoconus.," Am J Ophthalmol 108, 107-112 (1989).

22.   A. Tomidokoro, T. Oshika, S. Amano, S. Higaki, N. Maeda, and K. Miyata, "Changes in anterior and posterior corneal curvatures in keratoconus," Ophthalmology 107, 1328.1332 (2000).

23.   G. Smith, M. J. Cox, R. Calver, and L. F. Garner, "The spherical aberration of the crystalline lens of the human eye," Vision Res 41, 235-243 (2001).

24.   M. J. Mannis, J. Lightman, and R. D. Plotnik, "Corneal topography of posterior keratoconus," Cornea 11, 351-354 (1992).

25.   H. Mohammad and H. Hashemi, "A quantitative corneal topography index for detection of keratoconus.," J Refract Surg 14(keraroconus), 427-436 (1998).

26.   N. Maeda, S. D. Klyce, M. K. Smolek, and H. W. Thompson, "Automated keratoconus screening with corneal topography analysis," Invest Ophthalmol Vis Sci 35, 2749-2757 (1994).

27.   J. Schwiegerling, "Cone Dimensions in Keratoconus using Zernike polynomials," Optom Vis Sci 74(Keratoconus), 963-969 (1997).

28.   L. N. Thibos, R. A. Applegate, J. T. Schwiegerling, R. Webb, and V. S. T. Members, "Standars for reporting the optical aberrations of eyes," Vision Science and its Applications. Tops Volume 35(2000).

29.   S. G. El Hage and F. Berny, "Contribution of the crystalline lens to the spherical aberration of the eye," Journal of the Optical Society of America 63, 205-211 (1973).

30.   M. A. Lagana, I. G. Cox, and R. J. Potvin, "The effect of keratoconus on the wavefront aberration of the human eye," Invest Ophthalmol Vis Sci (suppl) 41, S679 (2000).